Optimizing the Age of Information for Blockchain Technology With Applications to IoT Sensors

Arnau Rovira-Sugranes and Abolfazl Razi

Abstract-Blockchain is an emerging technology that uses distributed ledgers for transparent, reliable, and traceable information exchange among network nodes. Blockchain and its 3rd generation Tangle-based implementations quickly extend their territory beyond crypto-currency to a broad range of applications using fee-less transactions over the Internet of things (IoT). However, this technology suffers from sluggishness in consensusbased validation of information that restricts its applicability to time-sensitive applications such as smart health. In this letter, we propose an optimized policy for sampling rate by IoT sensors that utilize blockchain and Tangle technologies for their transmission with the goal of minimizing the age of information (AoI) experienced by the end-users, considering both processing and networking resource constraints. Simulation results confirm the efficacy of the proposed algorithm compared to the current fixedrate update policy. Further, a closed-form solution is obtained for the optimal sampling rate in a network of homogeneous IoT nodes as a benchmark system.

Index Terms—Blockchain, age of information, Internet of things, adaptive scheduling, information sampling.

I. INTRODUCTION

INTERNET OF THINGS (IoT) is an ecosystem of connected devices that extends Internet connectivity far beyond the human users to smart devices including sensors, actuators, processing units, and digital machines. IoT is known to be the underlying platform for a broad range of applications such as smart city, smart home, smart health, smart transportation, and many more yet to come [1].

Blockchain is a recent technology that is primarily used for bitcoin crypto-currency [2], but quickly extended its territory to IoT applications, since it brings new features of transparency, verifiability, and traceability of information to the networking methods. Also, tampering data is hard and there is no need for a central authorization center for secure information exchange due to using consensus-based validation methods [3]. The key idea is forming a chain of information blocks, where each block contains several transactions, and is appended to the chain after consensus-based validation. This approach eliminates the need for central authorities to check data integrity, and authenticity, even in an untrustworthy environment [4]. The benefits of blockchain are achieved at the cost of a slow update rate that undermines its scalability to larger systems. For instance, a block validation time is

Manuscript received September 27, 2019; accepted October 16, 2019. Date of publication October 25, 2019; date of current version January 8, 2020. This material was based upon the work supported by the National Science Foundation under Grant No. 1755984. This work is also partially supported by the Arizona Board of Regents (ABOR) under Grant No. 1003329. The associate editor coordinating the review of this letter and approving it for publication was C. Feng. (Corresponding author: Abolfazl Razi.)

The authors are with the School of Informatics, Computing and Cyber Systems, Northern Arizona University, Flagstaff, AZ 86011 USA (e-mail: abolfazl.razi@gmail.com).

Digital Object Identifier 10.1109/LCOMM.2019.2949557

about 10 minutes based on the proof-of-work (PoW) mining method in the Bitcoin crypto-currency [5]. Later on, several improved mining methods are proposed to accelerate the rate of information exchange in the 2nd generation of this technology [6]. However, it is recognized that the slow update rate is inherent to blockchain, where the information is stored as a chain of blocks. To solve this issue, in the third generation of this technology, blockchain is replaced with Tangle, a specific directed acyclic graph (DAG) structure, where each transaction validates two randomly-selected prior transactions before joining the Tangle that significantly accelerates the validation rate [7]. The most popular implementation of the 3rd generation tangle-based distributed ledger system is IOTA, which offers a fast, scalable, tamper-proof and quantumresistant information exchange mechanism among the nodes. IOTA eliminates transaction fees and accommodates both value transfer and value-less information exchange, which makes it a suitable platform for IoT applications [8].

Despite the aforementioned techniques to accelerate the validation process of IOTA, the information access rate can still be dramatically low if the information generation rate grows uncontrollably high. Also, IoT sensors with limited power and computation capacity can quickly run out of battery by validating prior transactions more frequently than necessary [9]. The limited communication bandwidth of access nodes should also be taken into account. On the other hand, the information update rate in IoT sensors should be proportionate to the actual and meaningful variations of the parameters under measurement [10]. For instance, one would need faster updates for patients' heart rate than their blood pressure in a smart health application. Most current works aim to accelerate the information validation rate by improving the mining/validation process. In this letter, we offer a new perspective to this problem and enhance the freshness of IoT data by regulating the information injection rate taking both processing and communication factors into account.

II. SYSTEM MODEL

Consider an IoT platform that consists of N IoT nodes $(n_1,n_2,...,n_N)$, a wireless network with K access nodes $(a_1,a_2,...,a_K)$ and C cloud-based computational resources, as depicted in Fig. 1. Each IoT node n_i connects through an access node $a_j=a(n_i)$ to the entire service network to make the last state of its parameters accessible to other nodes using Blockchain/IOTA transmission mechanism.

The age of information (AoI) is typically defined as the time span from the measurement epoch to the delivery of data to an intended destination [11]. This concept is a commonly used performance metric to measure the freshness of data experienced by the end user that accounts for sampling delay, transmission latency, and the in-network computation times

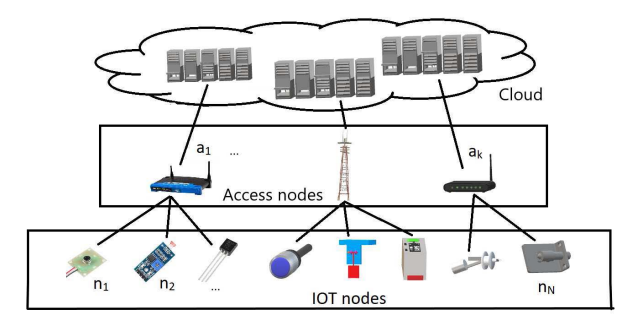


Fig. 1. Conceptual system model: layered IOTA network.

[12], [13]. Likewise, we define the AoI from the measurement epoch until the respective information propagates through the network and becomes accessible to the end users after getting validated by the blockchain/IOTA. The goal of the proposed optimization framework is to provide the network users with the most fresh information under communication and computation constraints.

We assume that each node n_i has a time-varying information vector $S_i(t) = [S_{i1}(t), \ldots, S_{iL_i}(t)]$, where each element $S_{ij}(t)$ refers to a parameter of type $j \in \{1, 2, \ldots, L_i\}$ at time point t. For example, if $S_i(t)$ is the inventory of a store in smart city, then $S_{ij}(t)$ can represent the number of products of type j in store i at time t. Each information source j changes independently at time points $\alpha_k^{(ij)}$, $k \in \{1, 2, 3, \ldots\}$ under a Poisson process of rate λ_{ij} ; Equivalently, the interval between two consecutive changes of S_{ij} follows an exponential distribution, i.e. $\Gamma_k^{(ij)} = \alpha_k^{(ij)} - \alpha_{k-1}^{(ij)} \sim Exp(\lambda_{ij})$ with expected value $1/\lambda_{ij}$. Measurements for node n_i are taken at time points $\beta_k^{(i)}$, with exponentially distributed measurement intervals $\Omega_k^{(i)} = \beta_k^{(i)} - \beta_{k-1}^{(i)} \sim Exp(\tau_i)$ with expected value $1/\tau_i$. Then, an information block I_k^i that contains fresh updates of all parameters until time point $\beta_k^{(i)}$ is pushed to the network and becomes available to the intended users at time point $\gamma_k^{(i)}$ after undergoing a random communication time $t_{c_k}^{(i)}$, and a random processing time $t_{v_k}^{(i)}$. Different time components are illustrated in Fig. 2.

III. OPTIMIZED AGE OF INFORMATION IN IOT

It has been shown that exponential distribution (i.e., $t_{c_k}^{(i)} \sim Exp(\eta_i)$) is a reasonable model for communication time (including the link establishment, actual transmission, and propagation through the network) in modern wireless communication infrastructures [14]. However, the mean time $(1/\eta_i)$ depends on the communication bandwidth of the access network. If an access node a_j covers a set of IoT nodes $\mathcal{A}_j = \{n_{j1}, n_{j2}, \dots, n_{jN_j}\}$, then its total bandwidth BW_j is assumed to be evenly split among the $\sum_{n_i \in \mathcal{A}_j} \tau_i$ active channel requests (note that the τ_i is the packet generation rate of node n_i). If P_L is the average length of an information packet, and r_c is the effective bitrate per unit bandwidth for the utilized networking technology, then the expected value

¹Note that we use exponential distribution for different time intervals (e.g., the time between two consecutive parameter changes, sampling interval, communication, propagation, and validation time in blockchain), following previous works and confirmed results [15]. However, arbitrary distributions with the same mean values can be used in our optimization framework based on the parameters under measurement, and the utilized communication infrastructure, and validation method.

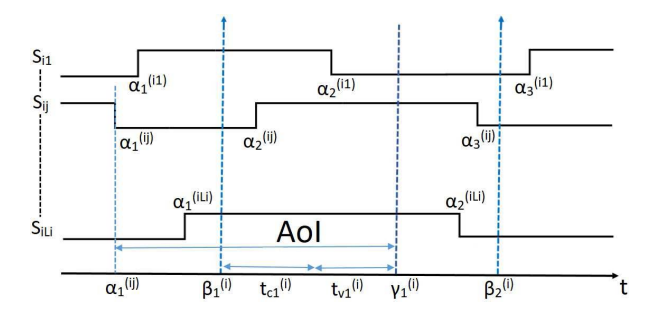


Fig. 2. Different components of the AoI for node n_i with parameters $S_{i1}, S_{i2}, \ldots, S_{iL_i}$.

of communication time for packets of user n_i , $1/\eta_i$ obeys the following constraint:

$$\mathbb{E}[t_{c_k}^{(i)}] = 1/\eta_i \ge \frac{P_L}{r_c B W_j / \sum_{n_i \in \mathcal{A}_i} \tau_i} = \frac{P_L \sum_{n_i \in \mathcal{A}_j} \tau_i}{r_c B W(a(n_i))}, (1)$$

where $BW(a(n_i))$ represents the bandwidth of $a(n_i)$, the access node serving IoT node n_i .

Likewise, the processing time is assumed to be an exponentially distributed random variable $tv_k^{(i)} \sim Exp(\zeta_i)$ with mean time $1/\zeta_i$ depending on the computational capability of the nodes that involve in the validation process. There is a clear distinction between the blockchain and Tangle technologies in this regard. To cover both technologies, here we take a general formulation that combines the computational power of volunteer miners (in blockchain) and sensor nodes (in IOTA). Let us assume that the computational power of each IoT node per unit time is c_i . In Tangle technology (like IOTA [8]), each node n_l provides verification service for two preceding transactions (i.e., it contributes $2c_l\tau_l$ computation resources) that yields a total computation power of $\sum_{l=1}^N 2c_l\tau_l$ for the entire network. Therefore, the expected value of validation time for transactions of node n_i follows:

$$\mathbb{E}[t_{v_k}^{(i)}] = 1/\zeta_i \ge \frac{r_v(\delta + \bar{\delta} \sum_{l=1, l \ne i}^{N} \tau_l)}{2 \sum_{l=1, l \ne i}^{N} c_l \tau_l} \approx \frac{r_v(\delta + \bar{\delta} \sum_{l=1}^{N} \tau_l)}{2 \sum_{l=1}^{N} c_l \tau_l}, \quad (2)$$

where $r_v(\delta + \bar{\delta} \sum_{l=1}^N \tau_l)$ is the expected required resources to validate a transaction in unit time. This includes two parts, a fixed amount of $r_v\delta$ and a second part $r_v\bar{\delta} \sum_{l=1}^N \tau_l$ that compensates for the probability of selecting a transaction for validation, noting the fact that this probability is inversely proportional to the total number of transaction $\sum_{l=1}^N \tau_l$. We use lower bound to consider computation overheads, and the approximation becomes equality when N is a large number. This provides the key advantage of scalability to Tangle-based methods since the computation time does not increase by adding more nodes to the network [16].

In the blockchain technology with PoW mining method (e.g., [4]), it is the opposite. The total cloud-based computation power of all miners C is evenly distributed among the active transactions $\sum_{l=1}^{N} \tau_l$. In this case, the average computation time is lower-bounded as

$$\mathbb{E}[t_{v_k}^{(i)}] = 1/\zeta_i \ge r_v \frac{\sum_{l=1}^N \tau_l}{C},\tag{3}$$

which obviously increases with the number of users and transaction rate; hence suffers from the scalability issue.

For instance, if $r_v=10^8$ is the required number of transactions for a transaction to get selected and validated by the network, and we have N=10 users with sampling rate $\tau=1$ packet per sec, then the total computation power of $r_v\sum_{l=1}^N \tau_l=10^9$ instructions is required to validate transactions in unit time. If the network mining power is $C=10^7$ instructions per second (IPS), then the mean validation time is about $10^9/C=10^7=100$ secs.

To cover both cases, we assume that a, $0 \le a \le 1$ controls the portion of processing powers of cloud-based servers versus IoT nodes. Then, we can combine (2) and (3) into:

$$\mathbb{E}[t_{v_k}^{(i)}] = 1/\zeta_i \ge r_v(\frac{(1-a)(\delta + \bar{\delta} \sum_{l=1}^N \tau_l)}{\sum_{l=1}^N c_l \tau_l} + \frac{a \sum_{l=1}^N \tau_l}{C}), \quad (4)$$

with a=1 for blockchain and a=0 for IOTA, as two extreme cases. The AoI includes the following components: (i) the time from parameter change to measurement epoch, (ii) communication time, and (iii) validation time. For information block I_k^i and parameter S_{ij} , it is defined as follows:

$$AoI(I_k^i, S_{ij}) = \gamma_k^{(i)} - \max\{\alpha_{k'}^{(ij)} | \alpha_{k'}^{(ij)} < \beta_k^{(i)} \}$$

$$= (\beta_k^{(i)} - \max\{\alpha_{k'}^{(ij)} | \alpha_{k'}^{(ij)} < \beta_k^{(i)} \}) + t_{ck}^{(i)} + t_{vk}^{(i)}$$
(5)

The first term in (5) is the time passed since the most recent parameter change $\alpha_{k'}^{(ij)} = \max\{\alpha_{k'}^{(ij)} | \alpha_{k'}^{(ij)} < \beta_k^{(i)}\}$ until the measurement epoch $\beta_k^{(i)}$. Each measurement epoch $\beta_k^{(i)}$ splits the interval between the two parameter change epochs $[\alpha_{k'}^{(ij)},\alpha_{k'+1}^{(ij)}]$ into two intervals $u=[\alpha_{k'}^{(ij)},\beta_k^{(i)}]$ and $v=[\beta_k^{(i)},\alpha_{k'+1}^{(ij)}]$. Since the measurement process $\{\alpha_1^{(ij)},\alpha_2^{(ij)},\ldots\}$ is independent of the parameter changes process $\{\beta_1^{(i)},\beta_2^{(i)},\ldots\}$, the cut point is uniformly distributed in $[\alpha_{k'}^{(ij)},\alpha_{k'+1}^{(ij)}]$ and we have $E[u]=E[v]=\frac{1}{2\lambda_{ij}}$. An alternative argument can be made considering the time-reversal property of parameter change epoch $\{\alpha_1^{(ij)},\alpha_2^{(ij)},\ldots,\alpha_k^{(ij)},\ldots\}$, and by reversing this process around time point $\beta_k^{(i)}$, we again obtain $E[\beta_k^{(i)}-\alpha_{k'}^{(ij)}]=E[\alpha_{k'+1}^{(ij)}-\beta_k^{(i)}]=\frac{1}{2\lambda_{ij}}$. Therefore, we have:

$$\overline{AoI}(I_k^i, S_{ij})] = \mathbb{E}[(\beta_k^{(i)} - \max\{\alpha_{k'}^{(ij)} | \alpha_{k'}^{(ij)} < \beta_k^{(i)}\}) + t_{ck}^{(i)} + t_{vk}^{(i)}] = \frac{1}{2\lambda_{ij}} + \frac{1}{\eta_i} + \frac{1}{\zeta_i}.$$
(6)

After averaging over all L_i parameters, we obtain the following expected AoI for the information packets of node n_i .

$$\overline{AoI}(n_i) = \frac{1}{2L_i} \sum_{j=1}^{L_i} \left(\frac{1}{2\lambda_{ij}} + \frac{1}{\eta_i} + \frac{1}{\zeta_i} \right).$$
 (7)

Finally, we note that it is desirable to set the measurement interval $1/\tau_i$ below the average information change interval $1/\overline{\lambda}_i = \frac{1}{L_i} \sum_{j=1}^{L_i} \frac{1}{\lambda_{ij}}$ to ensure that the majority of parameter changes are properly reported. Therefore, we impose the following constraint as well:

$$1/\tau_i \le 1/\overline{\lambda}_i = \frac{1}{L_i} \sum_{i=1}^{L_i} \frac{1}{\lambda_{ij}}.$$
 (8)

To minimize the average AoI for all nodes by controlling the vector of measurement rates $\tau = (\tau_1, \tau_2, \dots, \tau_N)$, we minimize Eq (7) subject to Eqs (1, 4, 8) as follows:

$$\tau^* = \underset{\tau}{\text{minimize}} \sum_{i=1}^{N} \left(\frac{(1/\overline{\lambda_i})}{2} + \frac{1}{\eta_i} + \frac{1}{\zeta_i} \right)$$

$$\text{subject to: } \eta_i \leq \frac{r_c BW(a(n_i))}{P_L \sum_{n_l \in \mathcal{A}_i} \tau_l}$$

$$\zeta_i \leq 1/\left(r_v \left(\frac{(1-a)(\delta + \overline{\delta} \sum_{l=1}^{N} \tau_l)}{\sum_{l=l}^{N} c_l \tau_l} + \frac{a \sum_{l=1}^{N} \tau_l}{C} \right) \right)$$

$$\tau_i \geq \overline{\lambda}_i,$$

$$\tau_i > 0, \quad \text{for } i = 1, 2, \dots, N$$

$$(9)$$

This problem does not seem to admit a closed-form solution but can be solved using numerical methods. To obtain insightful hints, we consider a homogeneous network where (i) all IoT and access nodes are uniform, and (ii) the association between the IoT and access nodes is uniform, meaning that for a network with K access nodes a_1, a_2, \ldots, a_K and N IoT nodes n_1, n_2, \ldots, n_N , each access node covers N/K nodes (i.e. $|\mathcal{A}_i| = N/K$). With these assumptions, we obtain the following simplified optimization problem:

$$\tau^* = \underset{\tau}{\text{minimize}} \frac{1}{2\lambda} + \frac{1}{\eta} + \frac{1}{\zeta}$$

$$\text{subject to: } \eta \le \frac{r_c K B W}{\tau N P_L}$$

$$\zeta \le 1/\left(r_v \left((1-a) \frac{(\delta + \bar{\delta} N \tau)}{N c \tau} + a \frac{N \tau}{C} \right) \right)$$

$$\tau \ge \bar{\lambda},$$

$$\tau > 0,$$

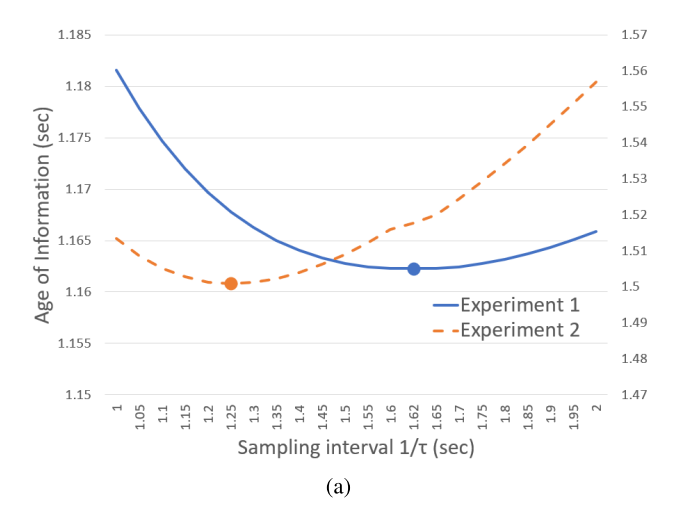
$$(10)$$

We observe that to minimize the term $1/\eta+1/\zeta=A\tau+B/\tau$ in the first two constraints, we need to choose $1/\tau=\sqrt{A/B}=\sqrt{\frac{aN^2c}{(1-a)(\delta+\bar{\delta}\sum_{l=1}^N\tau_l)C}}(1+\frac{P_LC}{aKr_cr_vBW}).$ Noting the other two constraints, we conclude that the minimizer of the objective function is

$$\tau^* = \max(\overline{\lambda}, 1/\sqrt{\frac{aN^2c}{(1-a)(\delta + \overline{\delta}\sum_{l=1}^N \tau_l)C}} \left(1 + \frac{P_LC}{aKr_cr_vBW}\right). \tag{11}$$

IV. SIMULATION RESULTS

In order to verify the validity of the optimization framework developed in section III, we obtain the optimal sampling rate τ from the optimization problem in (10) and compare it against the simulation results, as depicted in Fig. 3. Note that we use the mean sampling interval time $1/\tau$ in all figures. In this regard, we set up a network with uniform nodes and two different parameter sets shown in Fig. 3(b). First, we find the the optimal sampling interval $1/\tau^*$ in (11), which is 1.6227 and 1.2522, respectively for the two scenarios. Then, we execute intensive simulations with the given parameters and test values $1/\tau=1:0.05:2$ for both scenarios and plot the achieved average AoI curves. The simulation results suggest that the optimal values of the sampling interval is $\tau^*=1.62$ and $\tau^*=1.25$ for the two scenarios, respectively. It is interesting to see that the optimal values of $1/\tau$ obtained



Experiment 1	Experiment 2				
$a = 0.5, 1/\lambda = 2, \delta = 1$	$a = 0.5, 1/\lambda = 2, \delta = 1$				
N = 10, K = 3	N = 5, K = 1				
$BW = 20, P_L = 1$	$BW = 10, P_L = 1$				
C = 1000, c = 25	C = 220, c = 5				
$r_v = 25, r_c = 25$	$r_v = 10, r_c = 2.5$				
$\implies 1/\tau = $ 1.6227 sec	$\implies 1/\tau = $ 1.2522 sec				
(b)					

Fig. 3. a) Optimal sampling interval mean $1/\tau$ that minimizes the age of information. b) Optimal sampling interval: the solution of the optimization problem in Eq (11).

from the simulations closely match those offered by the analytical solution of the optimization problem in (10). In fact, they are the closest ones among the test values used for $1/\tau$ in the simulations. This perfect match between the simulation and analytical results confirms the validity of the developed analysis to optimize the AoI for IOTA/blockchain technology.

Also, a closer look at Fig. 3(a) confirms the expected valley-shaped curve for the AoI versus the sampling interval, $1/\tau$. For high values of $1/\tau$, the mean computation time $1/\zeta$ of IOTA $(a \to 0)$ increases due to the lack of sufficient validation resources, that in turn prolongs the average AoI. The upper limit for $1/\tau$ is determined by the average measurand update rate $(1/\tau \le 1/\overline{\lambda})$ as well. On the other hand, smaller values of $1/\tau$ mean more frequent packet injection to the system that can exceed the computation power of blockchain $(a \to 1)$ as well as the bitrate bottleneck of the access node that prolongs the AoI through increasing both mean communication time $1/\eta$ and mean computation time $1/\zeta$. The proposed policy has realized a reduction (up to a 10-fold) in the overall AoI, as seen in Fig. 4.

We analyze the impact of the number of IoT nodes N on the optimal sampling interval, $1/\tau$ in Fig. 4. As we see, the optimal $1/\tau$ increases with N. This means that we should inject fewer packets to the network in large-scale networks. Due to the limited bandwidth of access nodes, the share of bandwidth assigned to each IoT node decreases in larger networks, hence the longer communication intervals raise the overall AoI. To compensate for this effect, we need to lower down the sampling rate to produce less simultaneous requests by active IoT nodes.

Next, Fig. 5 analyzes the variation of the optimal sampling interval $1/\tau$ with the distribution of processing power between

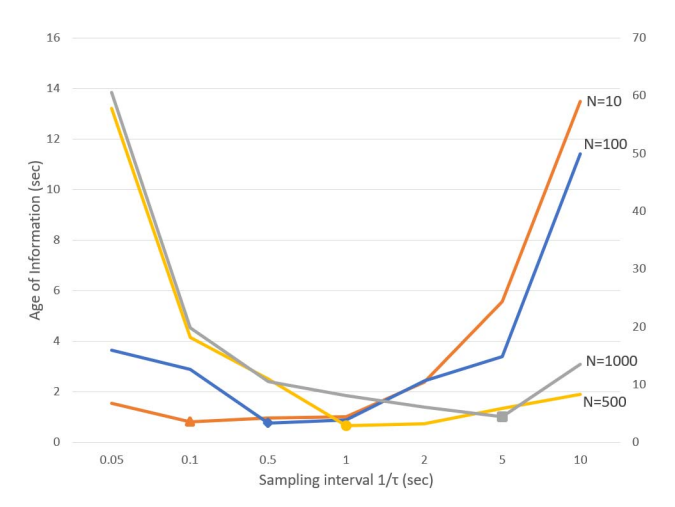


Fig. 4. AoI versus the sampling interval mean $1/\tau$ and number of IoT nodes N.

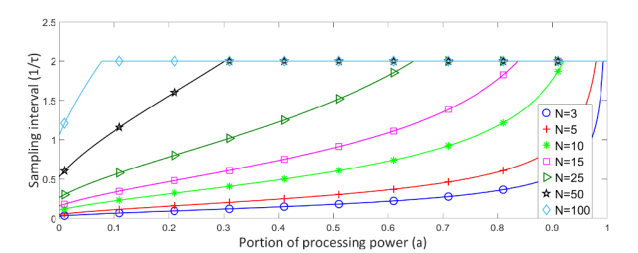


Fig. 5. Sampling interval mean $1/\tau$ for different values of portion of processing power a and the effect of changing number of IoT nodes N. $1/\lambda$ is set to 2.

the cloud-based servers and IoT nodes determined by parameter a. We observe that the optimal sampling interval increases with a, since larger values of a mean less involvement of IoT nodes in the validation process (i.e., in Blockchain), hence longer sampling intervals are required to avoid exhausting the fixed amount of cloud-based computation power. We also note that by increasing the number of IoT nodes N, the upper limit of mean sampling interval $1/\tau=1/\lambda$ is reached with lower values of a, which means that the bulk of the processing should be performed by IoT nodes when the network scales up. This confirms the fact that Tangle technology outperforms the blockchain technology in terms of processing efficiency in the next generation IoT with massive number of nodes.

Lastly, we evaluate the impact of the sampling rate on the achieved AoI for the more realistic case of nodes with heterogeneous characteristics. We obtain optimal sampling rates $[\tau_1, \tau_2, \dots, \tau_N]$ by solving the optimization problem in (9) using four different numerical optimization methods including particle swarm optimization (PSO), genetic algorithm (GA), simulated annealing (SA) and gradient descent (GD). First, we observe that different optimization methods consistently converge to the same solution and hence yield a similar average AoI for the whole system, that confirms the validity of the results. The results for a network with N=3 nodes are presented in Table I. We observe that for Blockchain (a = 1), the sampling rates converge to the limit $\tau_i \to \lambda_i$, whereas for Tangle (a = 0), we obtain different sampling rates, since increasing the transaction rate would increase the total available computation resources and hence reduce the average validation time t_v . Optimal rates depend on the node

TABLE I

Optimal Sampling Rate τ for Two Scenarios (a=0, and a=1) Using Different Optimization Methods. The Rest of Parameters are $N=3, K=1, C=10000, r_c=[5,10,8],$ $r_v=[500,400,800], BW=10, \lambda_i=[0.01,0.01,0.01],$ $P_l=[1000,500,300], \delta=0.5, c_i=[5,15,25]$

Scenario	Par.	PSO	GA	SA	SD
a = 0	$ au_1$	0.01	0.01	0.01	0.01
	$ au_2$	0.673	0.715	0.713	0.715
	$ au_3$	0.464	0.443	0.445	0.443
	AoI	80.373	80.344	80.344	80.344
	t_v	19.375	19.138	19.151	19.140
	t_c	10.998	11.206	11.193	11.203
a=1	$ au_1$	0.01	0.01	0.01	0.01
	$ au_2$	0.01	0.01	0.01	0.01
	$ au_3$	0.01	0.01	0.01	0.01
	AoI	50.289	50.291	50.289	50.289
	t_v	0.0017	0.0017	0.0017	0.0017
	t_c	0.287	0.289	0.287	0.287

TABLE II

Optimal Sampling Rate τ for Two Scenarios ($c_i=[50,15,10]$ and $\lambda_i=[1,0.04,0.1]$) Using Different Optimization Methods. The Rest of Parameters Are N=3,K=1,C=10000, $a=0,r_c=[5,5,5],rv=500[1,1,1],BW=10,\delta=0.5$ With $\lambda_i=0.01[1,1,1]$ and $P_l=1000[1,1,1]$ for the First Scenario and $c_i=10[1,1,1]$ and $P_l=1000[1,1,1]$ for the Second Scenario

Scenario	Par.	PSO	GA	SA	SD	NOP
$c_i = [50,15,10]$	τ_1	0.261	0.258	0.258	0.258	0.213
	$ au_2$	0.356	0.373	0.374	0.373	0.213
	τ_3	0.01	0.01	0.01	0.01	0.213
	t_v	18.111	17.830	17.823	17.830	20.093
	AoI	80.851	78.286	79.255	80.256	83.056
	$ au_1$	1.008	1	1	1	0.385
$\lambda_i = [1,0.04,0.1]$	$ au_2$	0.040	0.042	0.045	0.042	0.385
	$ au_3$	0.138	0.103	0.100	0.103	0.385
	AoI	286.753	284.248	284.005	284.280	383.926

characteristics. This observation is consistent with the results in Fig. 5, where we justified this observation.

In order to assess the variation of optimal sampling rates with different node characteristics, the results of two different scenarios are presented in Table II. For each scenario, we obtain the optimal sampling rate by solving (9) and compare the results with the conventional method of using equal sampling rates with no optimization for all node (denoted by NOP in Table II). In order to realize a fair comparison between the optimized and un-optimized methods, we set $au_i = \frac{1}{N} \sum_{i=1}^{N} au_i^*$ for NOP. Table II, scenario 1 evaluates the impact of the nodes' computation resources c_i on the optimal sampling rate (τ_i^*) . In IOTA technology (a=0), nodes with higher c_i are assigned with higher sampling rates to offer more computation resources to the network to accelerate the validation process in Tangle structure, shown by t_v in the Table. In particular, the optimized sampling rate achieves an average t_v of about 17.9 sec that exhibits an improvement of about 11%over the unoptimized method with $\tau_1 = \tau_2 = \tau_3 = 0.213$ and $t_v = 20.1$ sec. Likewise, scenario II investigates the impact of the parameter change rate λ_i on the sampling rate (τ_i^*) . As expected, the optimized method assigns higher τ_i^* for nodes with higher λ_i . The optimized method shows an improvement of 25% in the overall AoI for the optimized method.

V. Conclusion

In this work, we assess the concept of AoI in the IoT when using blockchain and Tangle technologies for transparent, reliable, and traceable information exchange. To the best of our knowledge, this is the first study that offers to adjust the information injection rate to optimize the average AoI based on the system configuration, processing power, and networking resources. Most other works try to implement faster mining/validation methods, ignoring the impact of networking factors. In particular, we confirmed the well-known superiority of Tangle over blockchain in terms of computation efficacy in large-scale networks. Our method offers a new guideline to adjust sampling rate for both blockchain and Tangle information exchange methods. The simulation results suggest an improvement of AoI by a factor of at least 10 compared to the current fixed-rate methods. We also find a closed-form solution for a special case of a network with homogeneous IoT nodes, as a benchmark reference for similar studies.

REFERENCES

- S. Poudel, "Internet of things: Underlying technologies, interoperability, and threats to privacy and security," *Berkeley Technol. Law J.*, vol. 31, no. 2, p. 997, 2016.
- [2] P. Vigna and M. J. Casey, The Age of Cryptocurrency: How Bitcoin and the Blockchain Are Challenging the Global Economic Order. New York, NY, USA: Macmillan, 2016.
- [3] M. Swan, Blockchain: Blueprint for a New Economy. Newton, MA, USA: O'Reilly Media, 2015.
- [4] M. Crosby, P. Pattanayak, S. Verma, and V. Kalyanaraman, "Blockchain technology: Beyond bitcoin," Appl. Innov., vol. 2, nos. 6–10, p. 71, 2016.
- [5] K. Croman et al., "On scaling decentralized blockchains (A position paper)," in Financial Cryptography and Data Security (Lecture Notes in Computer Science), vol. 9604. Berlin, Germany: Springer, 2016, pp. 106–125.
- [6] I. Bentov, C. Lee, A. Mizrahi, and M. Rosenfeld, "Proof of activity: Extending Bitcoin's proof of work via proof of stake," *IACR Cryptol. ePrint Arch.*, vol. 2014, p. 452, Dec. 2014. [Online]. Available: https://allquantor.at/blockchainbib/pdf/bentov2014proof.pdf
- [7] S. Popov, O. Saa, and P. Finardi, "Equilibria in the Tangle," Comput. Ind. Eng., vol. 136, pp. 160–172, Oct. 2019.
- [8] J. Shah and B. Mishra, "IoT enabled environmental monitoring system for smart cities," in *Proc. Int. Conf. Internet Things Appl.*, Jan. 2016, pp. 383–388.
- [9] F. Samie, V. Tsoutsouras, L. Bauer, S. Xydis, D. Soudris, and J. Henkel, "Computation offloading and resource allocation for low-power IoT edge devices," in *Proc. IEEE 3rd World Forum Internet Things*, Dec. 2016, pp. 7–12.
- [10] Z. Jiang, B. Krishnamachari, X. Zheng, S. Zhou, and Z. Niu, "Timely status update in massive IoT systems: Decentralized scheduling for wireless uplinks," 2018, arXiv:1801.03975. [Online]. Available: https://arxiv.org/abs/1801.03975
- [11] S. Kaul, R. Yates, and M. Gruteser, "Real-time status: How often should one update?" in *Proc. IEEE INFOCOM*, Mar. 2012, pp. 2731–2735.
- [12] A. Valehi and A. Razi, "Maximizing energy efficiency of cognitive wireless sensor networks with constrained age of information," *IEEE Trans. Cogn. Commun. Netw.*, vol. 3, no. 4, pp. 643–654, Dec. 2017.
- [13] I. Kadota, A. Sinha, and E. Modiano, "Optimizing age of information in wireless networks with throughput constraints," in *Proc. IEEE INFO-COM*, Apr. 2018, pp. 1844–1852.
- [14] R. R. Tyagi, F. Aurzada, K.-D. Lee, and M. Reisslein, "Connection establishment in LTE-A networks: Justification of Poisson process modeling," *IEEE Syst. J.*, vol. 11, no. 4, pp. 2383–2394, Dec. 2017.
- [15] J. Göbel, H. P. Keeler, A. E. Krzesinski, and P. G. Taylor, "Bit-coin blockchain dynamics: The selfish-mine strategy in the presence of propagation delay," *Perform. Eval.*, vol. 104, pp. 23–41, Oct. 2016.
- [16] S. Popov, "The tangle, version 1.3," White Paper, Oct. 2017.
 [Online]. Available: http://tanglereport.com/wp-content/uploads/2018/01/IOTA_Whitepaper.pdf